Effects of Amino Acid Substitutions on the Pressure Denaturation of Staphylococcal Nuclease As Monitored by Fluorescence and Nuclear Magnetic Resonance Spectroscopy†

Catherine A. Royer,*,‡ Andrew P. Hinck,§ Stewart N. Loh,§ Kenneth E. Prehoda,§ Xiangdong Peng,∥ Jiri Jonas,∥ and John L. Markley§

School of Pharmacy and Biochemistry Department, University of Wisconsin—Madison, Madison, Wisconsin 53706, and Department of Chemistry, School of Chemical Sciences, University of Illinois at Urbana-Champaign, Urbana, Illinois 61801

Received November 25, 1992; Revised Manuscript Received March 10, 1993

ABSTRACT: In the present study we have used high hydrostatic pressure coupled with either time-resolved and steady-state fluorescence or NMR spectroscopy in order to investigate the effects of amino acid substitutions on the high-pressure denaturation properties of staphylococcal nuclease. This protein has been shown previously to be structurally heterogeneous in its native state. On the NMR time scale, four distinct interconverting conformational forms arise from the population of both *cis* and *trans* Xaa–Pro peptide bonds (His^{46}–Pro^{47} and Lys^{116}–Pro^{117}) [Evans et al. (1989) *Biochemistry 28*, 362; Loh et al. (1991) *in Techniques in Protein Chemistry II*, pp 275–282, Academic Press, New York]. Mutations in the protein sequence have been shown to change the distribution among the various forms [Alexandrescu et al. (1989) *Biochemistry 28*, 204; Alexandrescu et al. (1990) *Biochemistry 29*, 4516]. Time-resolved fluorescence on a series of mutants with altered equilibria for *cis*/*trans* isomerism about the 116–117 peptide bond did not reveal any simple relationship between the position of the *cis*/*trans* equilibrium in the folded state and the heterogeneity of the fluorescence decay. However, the specific dynamic properties of each mutant, as revealed by time-resolved fluorescence, do appear to be correlated with their partial molar volume changes of denaturation. A striking finding is that mutation of either (or both) of the prolines that exhibits structural heterogeneity to glycine greatly alters the stability of the protein to pressure. These mutations also result in decreased chain mobility as assessed by time-resolved fluorescence. It appears that packing defects, which allow for peptide bond *cis*/*trans* heterogeneity in the wild-type protein, are removed by the Pro → Gly substitutions.

Staphylococcal nuclease (nuclease)[1] has been widely used as a model for understanding protein folding because it is a small (149 amino acid), single-domain monomeric protein that contains no sulfhydryl residues or disulfide linkages (Anfinsen, 1973). Nuclease undergoes reversible denaturation by a variety of perturbants including temperature, pH, and chemical denaturants. Upon denaturation by temperature, for example, nuclease exhibits a characteristic decrease in the fluorescence quantum yield of its single tryptophan residue (Shortle, 1986), as well as characteristic spectral changes in its histidine $^1H^{\epsilon 1}$ proton NMR signals (Evans et al., 1987). Whereas the global transition of nuclease appears to be generally two-state, NMR experiments have identified heterogeneity linked to cis/trans isomerization of prolyl peptide bonds in both the native and denatured states (Markley et al., 1970; Evans et al., 1987; Loh et al., 1991).

Site-specific amino acid substitutions in nuclease can cause large perturbations in the stability of the protein against denaturation, in the cooperativity of the unfolding transition, and in the degree of heterogeneity in the native state (Shortle et al., 1988; Fox et al., 1986; Alexandrescu et al., 1989, 1990). It is this last class of mutants that have been examined in the present work. The different conformational subspecies can be distinguished on the basis of NMR signals from the histidine $^1H^{\epsilon 1}$ protons. For folded nuclease, separate signals from His^8 and His^{121} report on the configuration, *cis* or *trans*, of the Lys^{116}–Pro^{117} peptide bond (Evans et al., 1987), and signals from His^{46} report on the configuration of the Lys^{46}–Pro^{47} peptide bond (Loh et al., 1991). The protein can fold from denatured states that have either *cis* or *trans* peptide bonds at Pro^{47} or Pro^{117} (Evans et al., 1987). Furthermore, the

† These studies were carried out with funding from the Graduate School of the University of Wisconsin to C.A.R. and from National Institutes of Health Grants RO1-GM35976 and RR02301 to J.L.M. and R01-GM42452 to J.J. and to Professor A. Jonas. A.P.H. was supported by Molecular Biophysics Training Grant GM08293, and S.N.L. was supported in part by Cell and Molecular Biology Training Grant 5 T32 GM07215.

* To whom correspondence should be addressed.
‡ School of Pharmacy, University of Wisconsin—Madison.
§ Biochemistry Department, University of Wisconsin—Madison.
∥ University of Illinois at Urbana–Champaign.

[1] Abbreviations: Bis-Tris, bis(2-hydroxyethyl)iminotris(hydroxymethyl)-methane; GuHCl, guanidine hydrochloride; $K_{U/F}(P)$, equilibrium constant for global protein unfolding (U, unfolded; F, folded) at a given pressure P; K_{tci}, equilibrium constant for the configuration at the $(i-1)-(i)$ peptide bond given by [*cis*]/[*trans*]; nuclease, staphylococcal nuclease; WT, recombinant protein produced in *E. coli* whose sequence is identical to that of the extracellular nuclease A from the Foggi strain of *Staphylococcus aureus*; H124L, recombinant protein produced in *E. coli* whose sequence is identical to that of the extracellular nuclease A from the V8 strain of *Staphylococcus aureus*; H124L+D77A, mutant of H124L in which asparate-77 has been replaced by alanine; H124L+F76V, mutant of H124L in which phenylalanine-76 has been replaced by valine; H124L+G79S, mutant of H124L in which glycine-79 has been replaced by serine; H124L+P47G, mutant of H124L in which proline-47 has been replaced by glycine; H124L+P117G, mutant of H124L in which proline-117 has been replaced by glycine; H124L+P47G+P117G, mutant of H124L in which prolines –47 and –117 have been replaced by glycine; NATA, *N*-acetyltryptophanamide; pH*, pH meter reading (calibrated by reference to standard buffers in H_2O) for a sample dissolved in ^2H_2O and uncorrected for the deuterium isotope effect on the glass electrode; ΔV°, change in the partial molar volume that accompanies the folded to unfolded transition.

0006-2960/93/0432-5222$04.00/0 © 1993 American Chemical Society

Table I: Results of Fluorescence Studies of the Pressure Unfolding of Staphylococcal Nuclease Variants[a]

sample	$\Delta V°$ (mL mol^{-1})	K_{tc117}	$\Delta G°$ (kcal mol^{-1}) pH 7.0	pH 5.5	pH 4.5	pH 3.5
WT	−92.2 ● 10	9	–	3.75	3.06	1.35
H124L+G79S	−84.6 ± 7	0.50	–	3.13	2.78	1.48
H124L+D77A	−89.9 ± 8	<0.01	2.30	0.54	0.17	–
H124L+F76V	−56.7 ± 8	0.83	–	1.02	0.69	

[a] $\Delta V°$ and $\Delta G°$ were calculated at P = 1 bar and T = 294 K from eq 1. Conditions were 10 mM Bis-Tris at 21 °C.

equilibrium among Xaa–Pro conformational states in folded (and presumably also in unfolded) nuclease depends on the solution conditions (Alexandrescu et al., 1989). The actual flux through various folding pathways thus depends upon solution conditions. For example, in wild-type nucleases the Lys^{116}–Pro^{117} peptide bond is predominantly *cis* at physiological temperature, but as the temperature is raised in a thermal unfolding experiment (carried out at equilibrium), the equilibrium shifts to the *trans* state (which is less stable) and unfolding proceeds predominantly from that state. Nonequilibrium folding and unfolding involves two-state conformational changes followed by establishment of Xaa–Pro peptide bond equilibria (Kuwajima et al., 1991; Sugawara et al., 1991; Shelongo et al., 1992). Recent kinetic studies comparing intrinsic tryptophan intensity and lifetime changes also provide evidence for an intermediate refolding form (Beechem, personal communication). We have examined here the pressure denaturation of two "wild-type" proteins, WT (Foggi strain nuclease) and H124L (V8 strain nuclease) and a number of mutant forms of the V8 nuclease. These proteins were selected because they exhibit different values for the *cis*/*trans* equilibrium about the 116–117 peptide bond:

$$116\text{–}117(trans) \overset{K_{tc117}}{\rightleftharpoons} 116\text{–}117(cis)$$

$$K_{tc117} = \frac{[116\text{–}117(cis)]}{[116\text{–}117(trans)]}$$

The K_{tc117} values for the proteins studied are shown in Table I.[2] The proteins studied have similar values of K_{tc47}, the *cis*/*trans* equilibrium about the peptide bond preceding proline 47, of approximately 0.25. Additionally, the mutant protein H124L+P47G was studied, which has K_{tc47} approximately equal to 0.[3]

The packing and dynamics of the protein matrix might be expected to differ for mutant proteins exhibiting different degrees of heterogeneity about these prolyl peptide bonds. Therefore, we used time-resolved fluorescence intensity and anisotropy to probe the dynamic properties of the single tryptophan residue (W^{140}) in the wild-type variants and in a series of mutants. Since polymer dynamics is related to free volume (Weber et al., 1984; Scarlata et al., 1984; Rholam et al., 1984), we also used high hydrostatic pressure to probe for differences in the change in partial molar volume of denaturation ($\Delta V°$) for these proteins as monitored by fluorescence and NMR spectroscopy.

MATERIALS AND METHODS

Mutagenesis. Site-directed mutants of H124L were generated by first inserting the entire plasmid encoding the protein (pTSCNcc; Wang et al., 1990) at its unique *Hin*dIII site into M13mp18. After preparation of single-stranded uridine-substituted DNA, site-directed mutagenesis was performed by the method of Kunkel et al. (1987) as described in Ausubel et al. (1987). For the primer extension reactions, we obtained the best results by using *Sequenase* Version 1.0 (USB, Cleveland, OH) and Pharmacia ultrapure dNTPs (Piscataway, NJ). DNA sequencing of single-stranded M13 recombinant DNA, as described in the *Sequenase* manual (Version 2.0), confirmed the results of the mutagenesis. Mutant overexpressing plasmids were recovered by first preparing double-stranded recombinant M13mp18 DNA, followed by digestion with *Hin*dIII. The 4.8-kb band corresponding to mutant linearized plasmid was obtained by extraction from low melting point agarose (Fischer Scientific, Co., Pittsburgh, PA) by the procedure outlined by Sambrook et al. (1989). All mutants were confirmed by double-stranded DNA sequencing of the recombinant overproducing plasmids.

Protein Purification. Wild-type and mutant nucleases were obtained by transforming the appropriate T7 overexpression vector into competent BL21(DE3) cells containing plasmid pLysS. Overproduction of the enzyme was achieved by growing 5 mL of this strain to log phase in LB medium and by inoculating this into 1 L of LB medium contained in a 2.8-L Fernbach flask. This culture was grown to late log phase, and overproduction was initiated by the addition of isopropyl β-D-thiogalactopyranoside (IPTG) to 0.01%. The cells were grown an additional 3 h and collected by centrifugation. The cell pellets were taken up in 0.1 volume of 0.1 M Tris base with 5 mM disodium ethylenediaminetetraacetate (EDTA) and 50 μM phenylmethanesulfonyl fluoride (PMSF). The cell pellets were frozen at −20 °C and then thawed slowly at room temperature. $CaCl_2$ was added to the lysed cell suspension to a final concentration of 10 mM (at which point the visocisity decreased dramatically), and the mixture was incubated 30 min at room temperature.

The precipitate that formed was removed by centrifugation, and the cleared lysate was passed through a 2.5-cm × 12-cm column of A50 DEAE-Sephadex equilibrated with 0.1 M Tris–glycine, pH 9.2. The column was washed with 2 column volumes of the same buffer, and the eluant was loaded directly onto a 2.5-cm × 12-cm column of C25 CM-Sephadex, which had been equilibrated with the same buffer. The column was then washed with 20 bed volumes of the same buffer followed by an additional 20 bed volumes of 0.2 M Tris-HCl, pH 7.6. The protein was eluted with 0.5 M Tris-HCl, pH 7.6, containing 1.0 M NaCl. It was dialyzed three times against 6 L of 0.3 M NaCl and then four times against double-distilled water. The sample was lyophilized as a white, salt-free powder.

Fluorescence Measurements and Analysis. Measurements were performed in 10 mM Bis-Tris at 21 °C unless otherwise indicated. Samples were prepared for fluorescence by dissolving approximately 1 mg of lyophilized nuclease in 1 mL of 10 mM Bis-Tris at the designated pH. The solutions were then diluted 10-fold into the same buffer. Exact concentrations, which were calculated from the absorbance at 280 nm

[2] That $K_{tc117} \approx 0$ for H124L+P117G was inferred from the fact that only a single $^1H^{\epsilon 1}$ signal was observed for His^8 and His^{121} of this mutant plus results from the X-ray structure of P117G, which shows a *trans* Lys^{116}–Pro^{117} peptide bond (Dr. R. O. Fox, personal communication).

[3] That $K_{tc47} = 0$ for H124L+P47G was inferred from the single $^1H^{\epsilon 1}$ signal observed for H^{46} in this mutant.

by using an extinction coefficient of 18 050 cm^{-1} M^{-1}, were always between 1 and 10 μM.

Steady-state fluorescence measurements were made with an ISS Koala spectrofluorometer (ISS, Urbana, IL) with 295-nm exciting light and 8-nm slit width. Emission spectra were monitored with 8-nm band-pass from 310 to 450 nm, while single-point intensity measurements were acquired using a long-wavelength-pass UV 340 filter from Hoya Optics (Sunnyvale, CA). Time-resolved measurements were made with the ISS multifrequency acquisition electronics. Excitation at 295 nm was obtained from the frequency-doubled cavity dumped output of a Coherent 701 R6G dye laser pumped by a mode-locked, frequency-doubled Coherent Antares Nd–YAG laser (Coherent Corp., Palo Alto, CA). The lamp excitation was coupled from the monochromator to the high-pressure cell or Koala sample compartment with a rectangular to circular optical fiber bundle (Oriel Corp., Stratford, CT). The laser excitation was directed into the high-pressure cell by means of UV-grade mirrors. A portion of the exciting light was partitioned off prior to its entering the high-pressure cell with a UV-grade beam splitter and directed into the reference photomultiplier tube of the Koala sample compartment, thus providing the trigger for the phase meter. For steady-state high-pressure fluorescence data acquisition, the filter detection optics and photomultiplier tube of the Koala were placed directly at the output window (90° from the excitation window, while the other two windows were blocked). For the time-resolved high-pressure fluorescence measurements, a monochromator was placed in the emission light path, and the reference lifetime (of 0 ns) was measured from the scattered exciting light with the emission monochromator automatically toggled between 340 nm (for sample) and 295 nm (for reference).

Time-resolved fluorescence data were analyzed, either in terms of discrete components or lifetime distributions in the single curve or global mode, by using the program Globals Unlimited (LFD, Urbana, IL). Errors in the phase measurement were taken as ±0.2° while the modulation error was assumed to be ±0.004 modulation units. Steady-state high-pressure denaturation profiles were analyzed for the free energy of unfolding and the associated volume change by using a modified version of the global biomolecular equilibrium analysis program BIOEQS (Royer et al., 1991; Royer & Beechem, 1992; Royer, 1993). In order to fit a folded-monomer to unfolded-monomer model, the numerical solver (EQS) was replaced by the closed-form analytical expression for the monomer unfolding equilibrium. The error was taken to be the square root of the total counts. Confidence limits of 67% on the values of the recovered $\Delta V°$ values were calculated by performing complete minimizations at each tested value of the parameter and by recording the χ^2 value obtained. In the analysis, all other parameters in the fit, in our case $\Delta G°$ and the intensities of the fully folded and unfolded forms, were allowed to vary. The 67% confidence level was calculated by using the numerical methods F-statistic program given the degrees of freedom and global χ^2 of the fit. These confidence limits represent the most rigorous evaluation of the error in the fit of the data that can be attained (Beechem, 1992).

NMR Measurements. Protein samples for NMR spectroscopy in ^2H_2O were prepared by first dissolving enough lyophilized salt-free protein in 3.0 mL of 99.99% ^2H_2O (Isotec Inc., Miamisburg, OH) to make the final protein concentration between 3 and 5 mM. Bis-Tris buffer (10 μL of 0.5 M in ^2H_2O) and maleic acid as an intensity standard (15 μL of 0.5 M in ^2H_2O) were added; the samples were heated at 50 °C for 1 h to exchange backbone amide protons with deuterons, and then the samples were lyophilized. Each sample was dissolved in 3.0 mL of 99.99% ^2H_2O, and the pH* was adjusted to 5.00 with 1 M ^2HCl or 1 M KO^2H as necessary. The sample was lyophilized again and finally dissolved in 99.997% ^2H_2O (Cambridge Isotope Laboratories, Cambridge, MA). The protein concentration was checked by measuring absorbance at 280 nm, and the pH* was determined by glass electrode measurement. Each of the samples contained 25 mM Bis-Tris and 5 mM maleic acid. The protein concentrations and pH* values differed slightly: H124L was 5 mM at pH* 5.15, WT was 4.4 mM at pH* 5.03, and H124L+G79S was 3.4 mM at pH* 5.11.

NMR spectra were acquired with a GE GN-300 spectrometer operating at 300 MHz and equipped with a custom-built, high-pressure, high-resolution ^1H NMR probe (Jonas et al., 1993). The temperature of the sample was monitored by a thermocouple inside the high-pressure vessel. Temperature control was provided by circulating cooling/heating fluid through a thermostatic jacket built into the probe. Spectra were acquired without ^2H lock and were digitized into 4K complex point arrays. The pulse sequence employed a relaxation delay of 3.0 s and a 60° pulse (50 μs). The sweep width was ±1501.5 Hz. Spectra at each pressure were acquired by collecting sets of 4–8 blocks, each with 64 scans, to minimize any effects of magnetic field drift. Twenty minutes was allowed between pressure changes to allow the system to reach equilibrium.

The data were transferred to a Silicon Graphics Personal Iris workstation and were converted from the 20-bit GE format to the 32-bit format used by the FELIX (Hare Research Inc., Woodinville, WA) NMR processing package. The data were Fourier-transformed with 1 Hz of exponential line broadening and were phased. The region containing the histidine $H^{\epsilon 1}$ resonances was written to an ASCII file suitable for input into the PEAKFIT (Jandel Scientific, Corte Madera, CA) peak deconvolution program. The individual resonances corresponding to native and denatured nuclease were fitted to Lorentzian line shapes, and their ratios gave the equilibrium constant for unfolding, $K_{U/F}$, as a function of pressure. For a two-state transition, $K_{U/F}(P)$ has the form of an increasing exponential (Weber & Drickamer, 1983):

$$K_{U/F}(P) = K_{U/F}(\text{atm}) \exp(-P\delta V°/RT) \qquad (1)$$

where

$$\Delta V° \equiv \left(\frac{\partial \Delta G°}{\partial P}\right)_{T,\text{pH},\ldots} = -RT\left(\frac{\partial \ln K}{\partial P}\right)_{T,\text{pH},\ldots} = \bar{V}°_U - \bar{V}°_F$$

The $K_{U/F}$ values calculated from the data were fit to eq 1 by using the nonlinear regression algorithm available in the SIGMAPLOT program (Jandel Scientific).

RESULTS

Dynamic Characterization of the Folded and Unfolded States by Fluorescence. It is known that, upon unfolding by pH, temperature, or guanidine hydrochloride (GuHCl), the intrinsic tryptophan fluorescence lifetime of nuclease decreases dramatically (Eftink et al., 1991a). The region of the protein structure surrounding W140 is shown in Figure 1 (top). Of particular interest are Lys^{133} and Lys^{110}, which are close to the tryptophan residue. The ϵ-amino group of Lys^{133} is positioned approximately 5 Å from the tryptophan indole ring, whereas that of Lys^{110} is at a distance of 9 Å. Although these distances (and the orientations) are not optimal for quenching

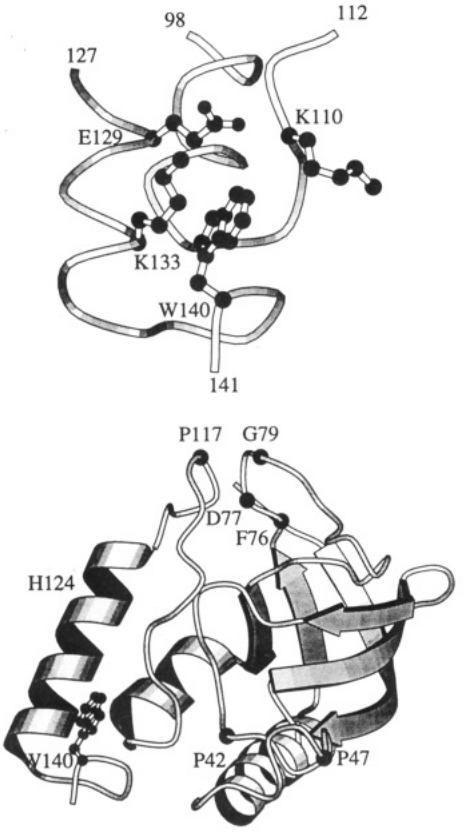

FIGURE 1: (Top) Polypeptide region of staphylococcal nuclease surrounding tryptophan 140. Note that the ε-amino group of Lys^{133} is within 5.24 Å of the indole ring. (Bottom) Ribbon diagram with the single site substitutions labeled. These figures were prepared with the MOLSCRIPT software package (Kraulis, 1991).

of the fluorescence emission of the tryptophan, increased mobility of the tryptophan or one or both of the lysines upon unfolding could allow contact between the π electron system of the indole ring and one of the amino groups, thereby resulting in collisional quenching through excited-state encounters. Fluorescence quenching for unfolded nuclease would thus be dependent upon the dynamic properties of the molecule. Fluorescence anisotropy decay measurements on native wild-type nuclease at room temperature have demonstrated that there is very little motion of the tryptophan residue on the 10–40-ps time scale (Eftink et al., 1991a); this result is consistent with the small degree of dynamic quenching of the tryptophan residue observed in the folded protein.

The fluorescence lifetime of the intrinsic tryptophan residue in WT nuclease has been shown to be insensitive to the state of isomerization (*cis* or *trans*) about the Lys^{116}–Pro^{117} peptide bond (Eftink et al., 1989). In order to investigate this in greater detail, we have measured the frequency response of the fluorescence emission for a series of nuclease mutants at pH 5.5. The amino acid substitutions investigated were either Pro to Gly substitutions at residues 47 and/or 117 or other substitutions that are known to alter K_{tc117}, the cis–trans equilibrium about the Lys^{116}–Pro^{117} peptide bond in the folded protein (Alexandrescu et al., 1990; Hinck et al., 1993). Figure 1 (bottom) shows a ribbon diagram of WT with the positions of single amino acid substitution labeled.

We have analyzed the fluorescence decay of these proteins in terms of a double exponential (Figure 2a). Regardless of the analysis scheme used (linked or unlinked lifetime, distributions or discrete decays), replacement of a proline with a glycine yields an increased average lifetime as compared to the parent H124L. By contrast, the lifetimes obtained for H124L+G79S and H124L+D77A (measured at pH 7) were shorter. H124L+F76V also exhibited a longer lifetime than H124L. The values of the recovered lifetimes were comparable for each mutant if each curve is analyzed individually. However, when we carried out a global analysis in which we linked the value of the two lifetimes among the data sets for all of the mutants, we obtained slightly higher χ^2 values but nonetheless reasonable fits with 5.7 and 2.2 ns as the values of the two components. The fraction of molecules emitting with the longer lifetime is larger for the proline to glycine mutants than for all other variants except F76V (Figure 2b).

In analogy with the analysis of several other single tryptophan proteins (Alcala et al., 1987; Chen et al., 1987; Hutnik et al., 1989; Stayton & Sligar, 1991; Atkins et al., 1991; Kim et al., 1993), we interpret the heterogeneity of the fluorescence decay in nuclease as arising from two conformational substates of the environment surrounding the tryptophan residue which interconvert on a time scale that is slow compared to the fluorescence decay. In the less populated state, the one with the 2.2-ns lifetime, dynamic quenching of the tryptophan fluorescence is more efficient, indicating greater mobility of the surrounding protein matrix. This more mobile state is less populated in the proline to glycine mutants and in H124L+F76V than in H124L. By contrast, the conformation is more populated in mutants H124L+G79S and H124L+D77A than in H124L.

We also measured the frequency response of the differential polarization of the intrinsic fluorescence in order to characterize the time-resolved anisotropy of Trp^{140} in the different proteins. In all but H124L+D77A, we found that the best fit to the data was to a single rotational correlation time of about 11 ns (Figure 2c). No local motion of the tryptophan could be detected with frequencies up to 100 MHz, and the recovered limiting anisotropy (0.26) in all cases was quite close to the limiting value of 0.27 found for excitation at 295 nm of NATA in propylene glycol at low temperature (Valeur & Weber, 1977). This shows that these proteins exhibit very little fast motion of the tryptophan. Although small differences in the limiting anisotropy from that of free tryptophan can be induced by the surrounding protein matrix, this high recovered value for the limiting anisotropy plus the lack of any observed fast motion are consistent with a very rigid tryptophan moiety in the nuclease variants studied here. The tryptophan in WT exhibits a very small but detectable amount of fast motion (Eftink et al., 1991a). In Figure 2c, the frequency response of the differential polarization of H124L+D77A is compared to that of H124L. Significant fast tryptophan motion (30 ps) was evident. In addition, we found that the correlation time for H124L+D77A was slightly larger than for the others (12.2 ns at pH 7 and 13.3 ns at pH 5.5, compared to values between 11.0 and 11.7 ns at pH 5.5). These results imply that this mutant can assume conformations in which the structure is relaxed sufficiently so as to permit motions of the tryptophan and/or surrounding amino acid residues that lead to significant dynamic fluorescence quenching and rotational depolarization of fluorescence. Any tryptophan motions that would contribute to dynamic quenching of fluorescence in all of the proteins except H124L+D77A are apparently too fast or too small to be detected by these anisotropy decay experiments. On the other hand, quenching may result from motions of Lys^{133} or another quenching residue, in which case dynamic quenching would not be dependent upon motion of the tryptophan alone.

Pressure Denaturation of Nuclease and the Site-Specific Mutants As Monitored by Fluorescence. Since changes in

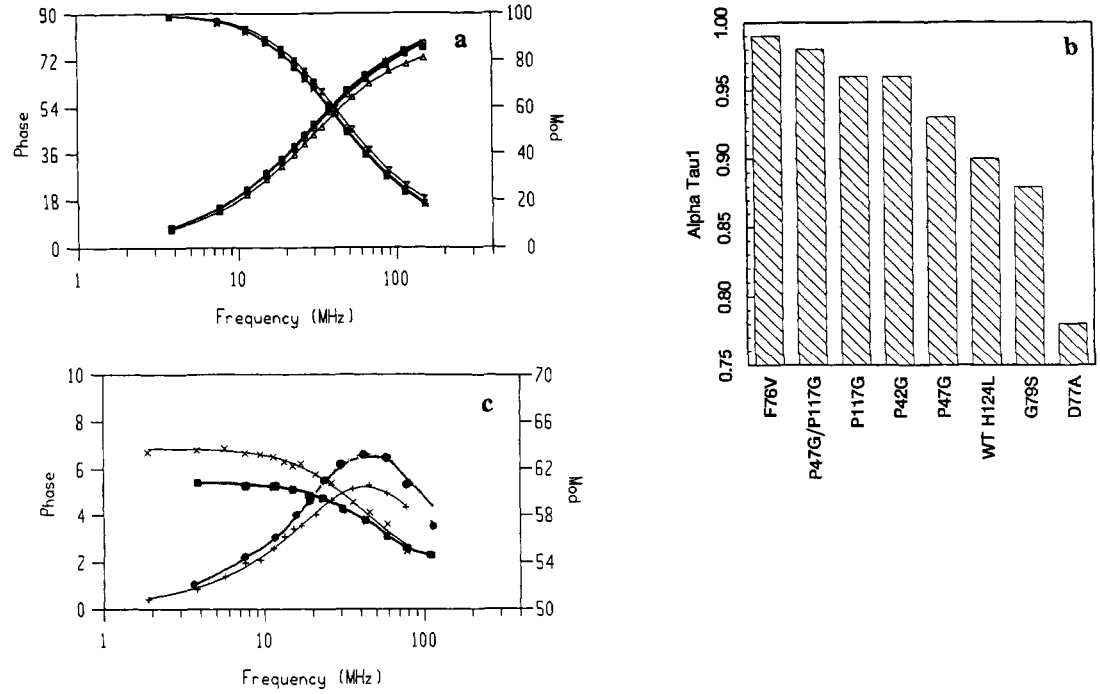

FIGURE 2: Fluorescence lifetime results on the V-8 strain nuclease (H124L) and mutants. (a) Frequency response profiles for H124L+P47G+P117G, H124L+P117G, H124L+P42G, H124L+P47G, H124L, 6-H124L+G79S, H124L+F76V, and H124L+D77A (Δ and ⧗). The fit is drawn through the data points. In this fit the lifetimes were linked across all data sets, except 7. The values of the recovered lifetimes were 5.7 and 2.2 ns, except for H124L+D77A, for which the values were 5.2 and 0.5 ns. (b) Relative population of molecules emitting with the long lifetime for each of the nuclease proteins. (c) Differential polarization for H124L (●, phase; ■, modulation) and H124L+D77A (+, phase; ×, modulation). Excitation was at 295 nm and emission was monitored for panel a with the emission monochromator set at 350 nm (8-nm band-pass) or for panel b with a WG 340 cuton filter.

the heterogeneity of the peptide bond between residues 116 and 117 appeared to influence the dynamic properties of the folded nuclease chain, we carried out high-pressure denaturation experiments on this series of mutants in order to ascertain whether these differences in dynamic properties could be correlated with differences in $\Delta V°$, the volume change of unfolding. Pressure denaturation profiles of WT at different pH values are shown in Figure 3a. These profiles were obtained by measuring the total steady-state fluorescence emission intensity (as monitored through a WG340 cuton filter) as a function of increasing hydrostatic pressure at four pH values from 5.5 to 2.6. All pressure denaturation profiles were 95–100% reversible upon release of pressure. The loss of fluorescence intensity observed upon decreasing the pH from 5.5 to 2.6 (low-pH unfolding) was similar in magnitude to that found upon increasing the pressure from 1 atm to 2.5 kbar (pressure unfolding). Another observation was that whereas the free energy of denaturation is obviously dependent upon pH (the pressure denaturation curves shift to lower pressures upon decreasing the pH), the volume changes (or slopes of the plots) showed very little pH dependence.

The pressure denaturation data in Figure 3a from the first three pH values (between 3.5 and 5.5) were analyzed simultaneously by using a global nonlinear analysis program for the pressure-induced unfolding of monomer as described in Materials and Methods. The value of $\Delta V°$ was linked across the three data sets, while the free energies of unfolding and the intensities of the folded and unfolded forms were allowed to vary. Unlinking of end points was allowed because the alignment of the high-pressure cell varies slightly between runs, such that small variations in the total measured intensity can occur. The lines through the points in Figure 3a correspond to the results of this analysis. The recovered volume change was −91.3 mL/mol. This value of −91.3 mL/mol is in good agreement with the results of Eftink and co-workers (Eftink et al., 1991b) on another mutant of nuclease. The global χ^2 (expressed as $1-\chi^2$) obtained was 0.78, and confidence limit testing of the volume change parameter yielded a symmetric χ^2 plot with 67% confidence limits at ±10 mL/mol. Unlinking of the $\Delta V°$ values did not improve the fit significantly. The independence of the volume change from the pH suggests that electrostriction of water around ion pairs that are disrupted upon unfolding contributes little to $\Delta V°$.

H124L (V8 strain nuclease A) is considerably more stable than WT (Foggi strain nuclease A) and was not denatured at the highest pressure achievable in the fluorescence cell. The less stable H124L+G79S, H124L+D77A, and H124L+F76V mutants, however, did undergo an unfolding transition within the available pressure range. The results of those experiments at a series of pH values are presented in Figure 3b–d. Except for pH values at which no change in the intensity was observed, the lines through the data points represent the results of global analysis of the different pH data sets: analysis in which $\Delta V°$ was linked across all pH values. As in the case of WT, the magnitude of the fluorescence intensity decrease with pressure was similar to that obtained with pH. Also, as in the case of WT, $\Delta V°$ showed little pH dependence, since unlinking the pH data sets did not improve the fits significantly. The partial molar volume changes and free energies of unfolding recovered from these analyses are given in Table I. The absolute value of the free energy of unfolding decreases at low pH, as one would predict. The volume changes of unfolding of H124L+G79S and H124L+D77A are not significantly different from that of WT: all are near −80 to −90 mL/mol. H124L+F76V, on the other hand, exhibited a $\Delta V°$ of −56 mL/mol, which is significantly smaller in absolute value than that observed for WT or the other mutants examined. H124L+F76V also displayed the greatest degree of homogeneity in its fluorescence decay (Figure 2b).

The pressure profiles for the Pro→Gly substitution mutants are shown in Figure 4. These mutants displayed behavior

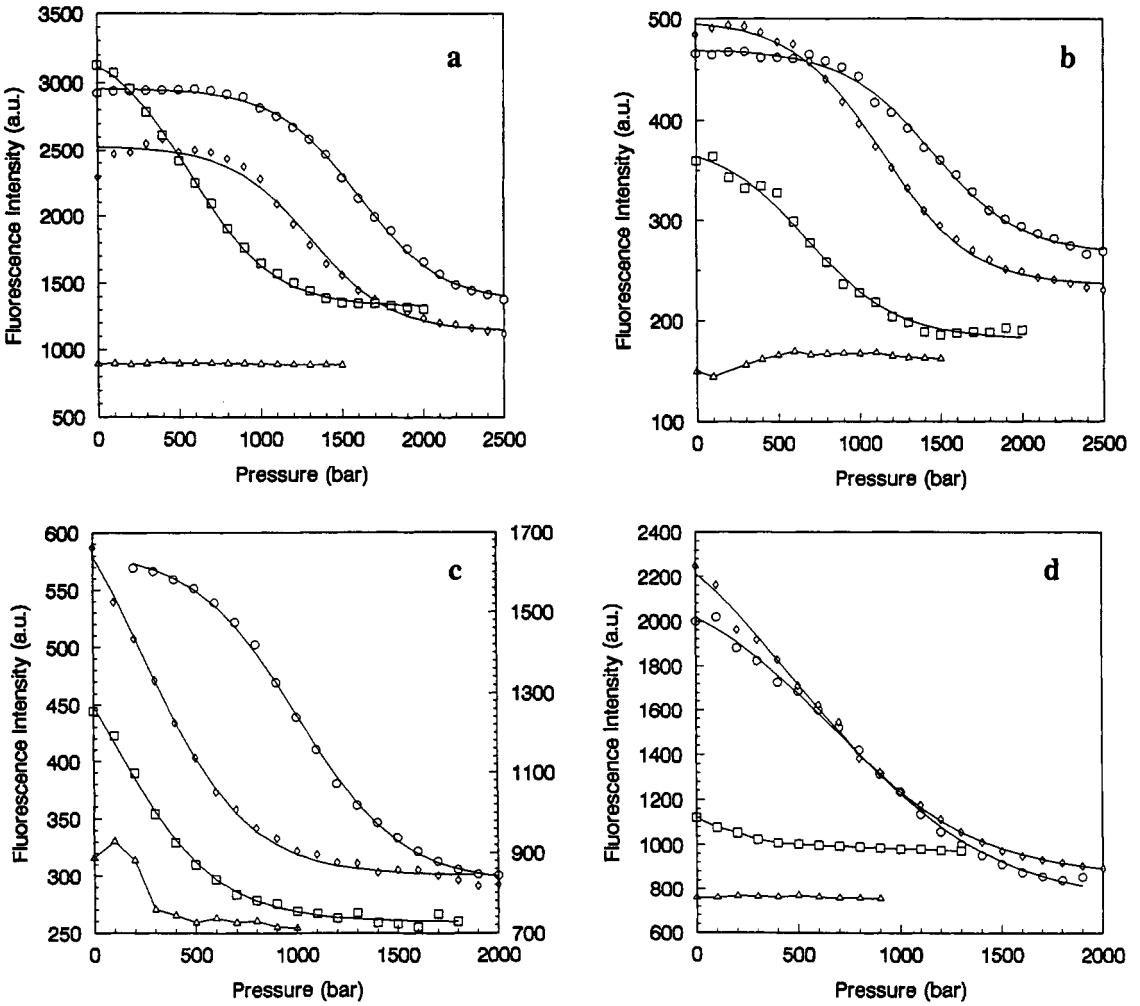

FIGURE 3: Pressure denaturation profiles as a function of pH from monitoring the total steady-state fluorescence intensity for (a) WT, (b) H124L+G79S, (c) H124L+/D77A, and (d) H124L+F76V. Lines through the data points represent fits to the data (see *Materials and Methods*), except where there was no effect of pressure on the intensity. Excitation was at 295 nm and emission was monitored with a WG 340 cuton filter. Symbols in panels a, b, and d correspond to (○) pH 5.5, (◇) pH 4.5, (□) pH 3.5, and (△) pH 2.6. Symbols in panel c correspond to (○) pH 7.0, (◇) pH 5.5, (□) pH 4.5, and (△) pH 3.5.

much different from that of the other mutants. H124L+P42G and H124L+P47G (Figure 4a,b) exhibited a pressure-dependent decrease in fluorescence intensity. Values of $\Delta V°$ from plots at pH 3.0, fitted as denaturation profiles (near −15 and −22 mL/mol), were much smaller than those for the other mutants. H124L+P117G exhibited essentially no effect of pressure over the range available in our high-pressure fluorescence system (data not shown). For the double proline to glycine mutant, H124L+P47G+P117G (Figure 4c), the pressure effect was reversed, in that the fluorescence intensity increased upon application of pressure. The small observed decrease in fluorescence intensity for the single proline to glycine mutants may also reflect a conformational change other than unfolding. Therefore, the $\Delta V°$ values for these mutants cannot be assigned conclusively to an unfolding transition. Relative quantum yield measurements of the various proteins were within experimental error for all of the nuclease mutants examined and thus did not indicate any increased static quenching effect in the native states of the proline to glycine mutants over the other nuclease variants examined.

The fluorescence frequency response profiles for WT, H124L+D77A, H124L+P42G, and H124L+P47G+P117G are plotted in Figure 5, panels a–d, respectively. Results are shown at atmospheric pressure (+, phase; ×, modulation) and at pressures at which the variants are largely unfolded (□, phase; ○, modulation) as determined from their steady-state profiles (Figures 3 and 4).

Figure 6 shows frequency response profiles as a function of pH. Large changes in frequency response curves of the kind seen upon pH denaturation were also observed upon temperature denaturation (Eftink et al., 1991a) or upon denaturation by GuHCl (Beechem, personal communication). On the other hand, pressure denaturation leads to much smaller changes (Figure 5), even though the extent to which the tryptophan emission intensity is quenched is quite similar to that observed upon decreasing the pH (Figures 3 and 4). These results demonstrate that, whereas the mechanism of tryptophan fluorescence quenching in the pH-, temperature-, and GuHCl-denatured states is predominantly dynamic in origin, that observed in the pressure-denatured state has a large static component. In the case of the double proline to glycine mutant (Figure 5d), no increase in fluorescence lifetime was observed upon application of high pressure. Since no change in the fluorescence lifetime was observed upon application of pressure, we conclude that that there is a certain degree of static quenching of the tryptophan in the native state of this protein. This may be true for WT and for other variants, as well. Application of pressure to the double proline to glycine mutant appears to result in the relief of static, rather than dynamic, quenching. The lack of a significant pressure effect on the fluorescence lifetime in all cases would suggest that

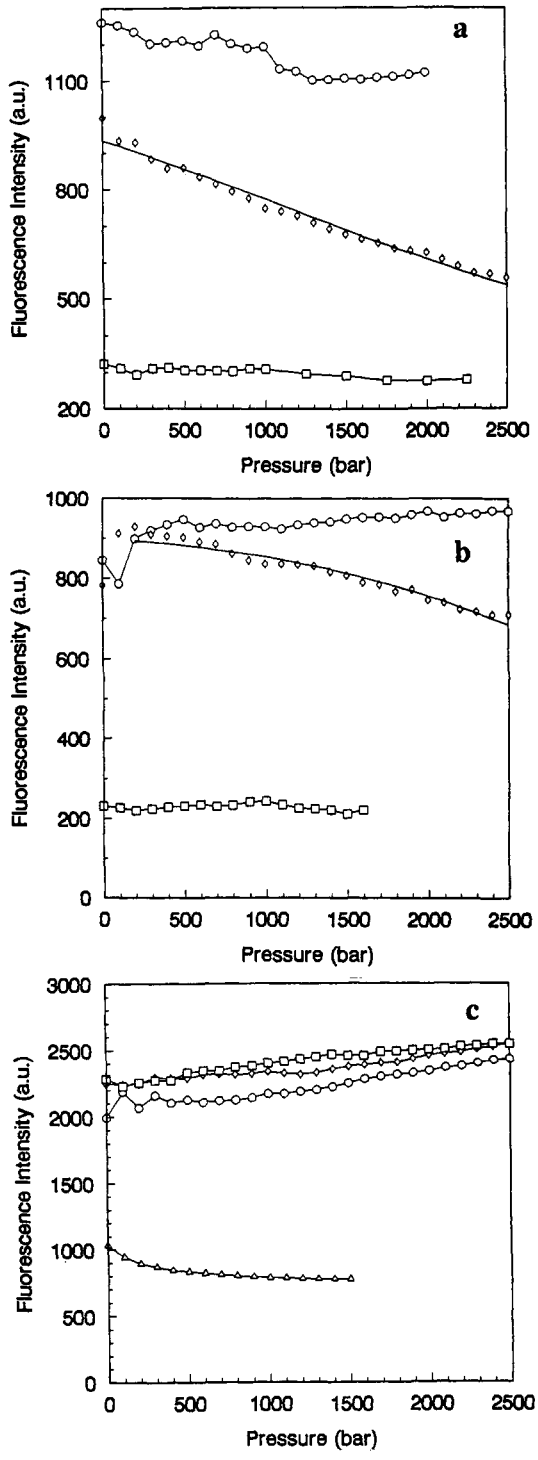

FIGURE 4: Pressure denaturation profiles as a function of pH monitoring the total steady-state fluorescence intensity for (a) H124L+P42G, (b) H124L+P47G, (c) H124L+/P47G+/P117G. Excitation was at 295 nm, and emission was monitored with a WG 340 cuton filter. Symbols in panels a and b correspond to (○) pH 4.5, (◇) pH 3.0, and (□) pH 2.6. Symbols in panel correspond to (○) pH 5.5, (◇) pH 4.5, (□) pH 3.5, and (△) pH 2.6.

there is less mobility of Trp^{140} in the pressure-denatured state than in the pH-denatured state and that Trp^{140} in the pressure-denatured state forms a ground-state complex with a quenching moiety, perhaps Lys^{133}. These results are in accord with those of Beechem (personal communication), who has also observed a statically quenched intermediate refolding species in pH-jump double kinetics (ns/ms) refolding studies in which both fluorescence lifetime and total intensity were monitored.

Pressure Denaturation of Nuclease As Monitored by NMR. The histidine $^1H^{\epsilon 1}$ region of the NMR spectrum of H124L+G79S as a function of pressure is shown in Figure 7a as an example of results of this kind obtained for all of the variants. These experiments were carried out in the same buffer as the fluorescence experiments but at a higher temperature (37 vs 21 °C) to increase resolution. The histidine spectrum obtained at high pressure is similar to that obtained upon temperature denaturation (Alexandrescu et al., 1990). The finding that lines are sharpened and that signals from individual residues of a given type (e.g., histidine) become equivalent indicates that the protein is fully unfolded at high pressure. Peak integrals corresponding to histidines in the unfolded state of the protein increase as a function of pressure at the expense of those corresponding to the folded state. These data corroborate those obtained from tryptophan fluorescence emission as a function of pressure. Since the histidine residues report on multiple regions in the protein that are distinct from the region of the tryptophan, the combined NMR and fluorescence results indicate that high pressure leads to global disruption of the structure. Figure 8 shows plots of the log of the ratios of histidine peak integrals from the folded and unfolded states as a function of pressure, $K_{U/F}(P)$, for WT, H124L, and H124L+G79S. Values of $\Delta G°$ and $\Delta V°$ for pressure denaturation, calculated from nonlinear least-squares fits of the data, are summarized in Table II. The high-pressure NMR results are consistent with the fluorescence results in that WT and H124L+G79S exhibited similar volume changes and free energies of unfolding. The $\Delta V°$ values recovered from the two approaches (NMR and fluorescence) were significantly different, however, as discussed below.

Since the NMR experiments were performed at 37 °C in ^2H_2O and the fluorescence was done at 21 °C in ^1H_2O, we repeated the high-pressure fluorescence studies of WT and H124L+G79S under conditions more like those of the NMR experiments: 99.9% ^2H_2O at pH* 5.5 and at 37 °C. The only differences in conditions in these experiments were the protein concentration (1–10 μM for fluorescence and 1–5 mM for NMR) and a slight pH* difference (0.4 pH unit higher in the fluorescence experiments). The results of fitting these data are given in Table III. For both protein variants, $\Delta V°$ diminished considerably in absolute value from near −80 to −90 mL/mol at 21 °C to near −55 mL/mol at 37 °C. These $\Delta V°$ values are similar to those recovered from the NMR data (Table II). The midpoints of the fluorescence high-pressure denaturation profiles were at slightly higher pressures than those of the NMR profiles, and the free energy changes were correspondingly larger in absolute value. These discrepancies in midpoint and free energy probably stem from the slight differences in the solution conditions; since the pH* of the NMR solution was 0.4 pH unit lower, one would expect the samples studied by NMR to be destabilized relative to those studied by fluorescence, as was observed.

The high-pressure NMR probe was capable of containing higher pressures (up to 5 kbar) than those available in the fluorescence experiments (up to 2.5 kbar). Denaturation of H124L, which showed no change in the range studied using fluorescence, could be evaluated by NMR. Its $P_{1/2}$ was near 3 kbar, and its $\Delta V°$ was −65 mL/mol, which is slightly larger than values found for WT and H124L+G79S (Table II). The stability of the double proline to glycine mutant, H124L+P47G+P117G, was such that its one-dimensional ^1H spectrum was unchanged up to 5 kbar.

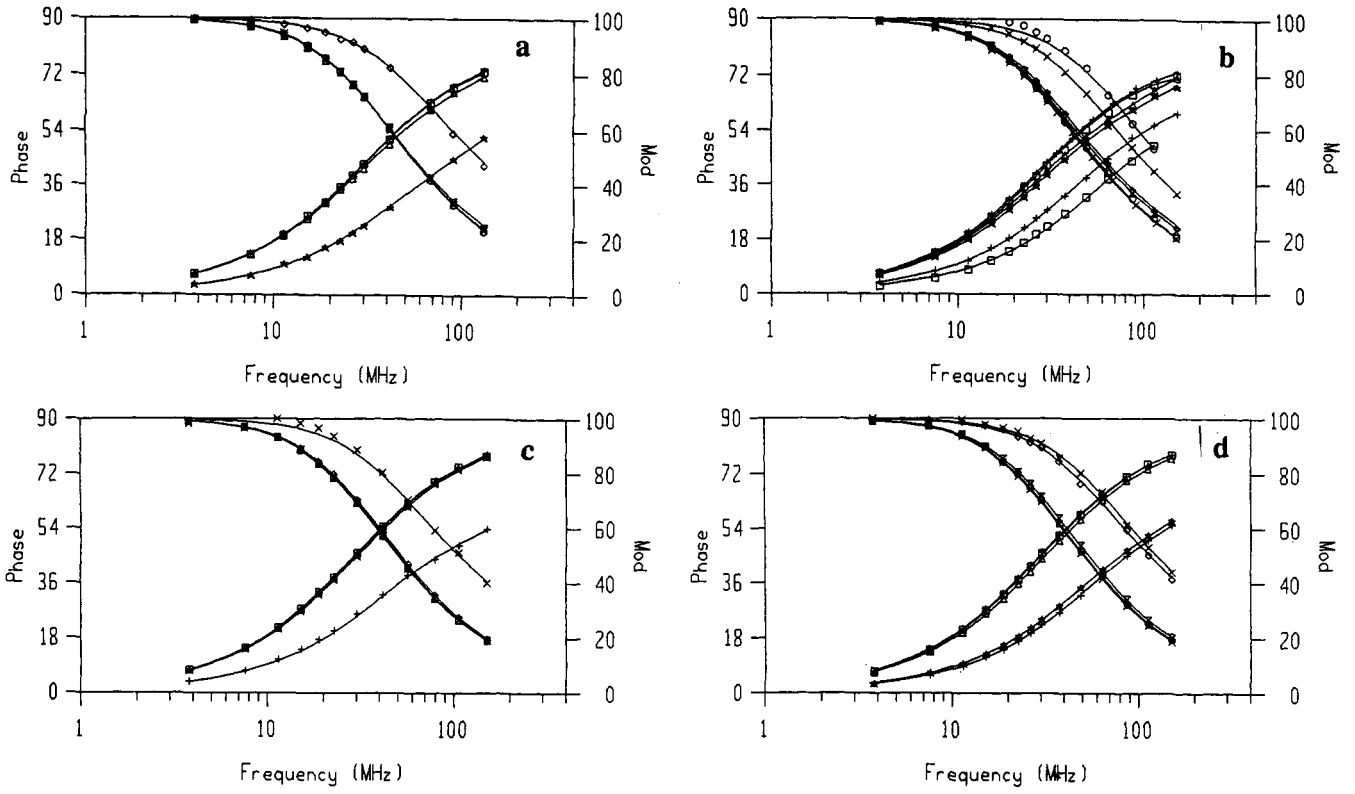

FIGURE 5: Effect of pressure on fluorescence lifetimes. Frequency response profiles at atmospheric pressure and at high pressure (either near the complete denaturation pressure or 2.0 kbar) are shown for (a) WT, pH 5.5 (atm and 2.0 kbar), (b) H124L+D77A, pH 5.5 (atm and 1.0 kbar), (c) H124L+p45G, pH 3.0 (atm and 2.0 kbar), and (d) H124L+P47G+P117G, pH 3.0 (atm and 2.0 kbar). Excitation was at 295 nm, and emission was monitored with the emission monochromator set at 350 nm (8-nm band-pass). Symbols are as follows: (+) atmospheric pressure phase data, (×) atmospheric pressure modulation data, (□) high pressure phase data, and (○) high pressure modulation data.

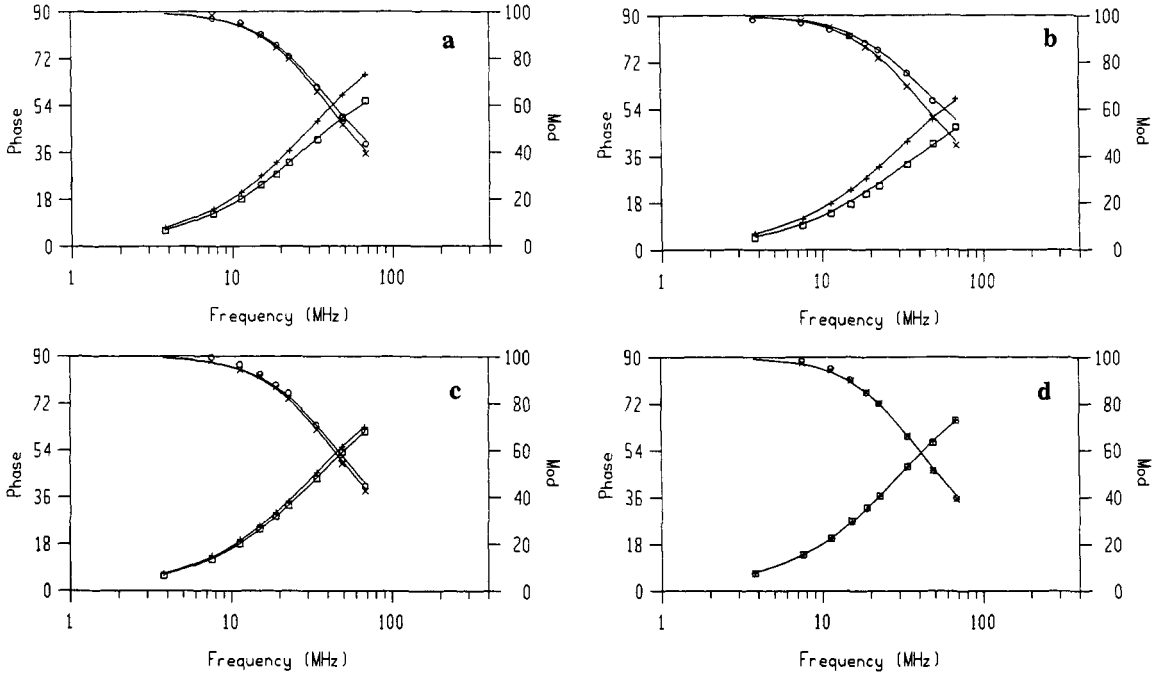

FIGURE 6: Effect of pH on fluorescence lifetimes. Frequency response profiles for (a) H124L (pH 5.0, 4.0, 3.0, and 2.6), (b) H124L+D77A (pH 7.0, 5.5, 4.5, 3.5, 3.0, and 2.5), (c) H124L+P42G (pH 5.5, 4.5, 3.5, 3.0, and 2.6), and (d) H124L+P47G+P117G (pH 5.5, 4.5, 3.5, 3.0, and 2.6) all at atmospheric pressure. Excitation was at 295 nm, and emission was monitored with the emission monochromator set at 350 nm (8-nm band-pass). Frequency response curves shift to higher frequency with decreasing pH.

DISCUSSION

The time-resolved fluorescence results for nuclease and the series of site-specific mutants reported here support the premise that the observed fluorescence decay parameters of Trp^{140} are linked to the dynamic properties of the particular mutant. The implication that Lys^{133} may be responsible for the quenching of Trp^{140} is supported by studies of Rudzki and Brand (personal communication), which demonstrate that replacement of Lys^{133} by Thr results in a decrease in the long-lifetime component. Rudzki and Brand found that replace-

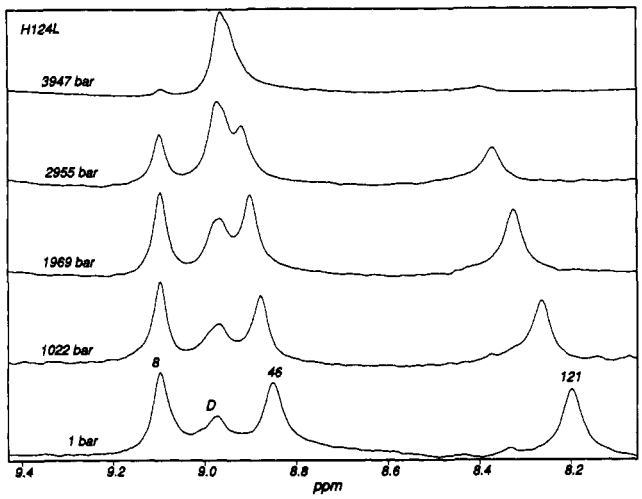

FIGURE 7: Histidine $^1H^{\epsilon 1}$ region of the proton NMR spectrum of H124L at atmospheric pressure and at 1.0, 2.0, 3.0, and 4.0 kbar. The protein concentration was 5.5 mM at pH 5.15 at 37 °C.

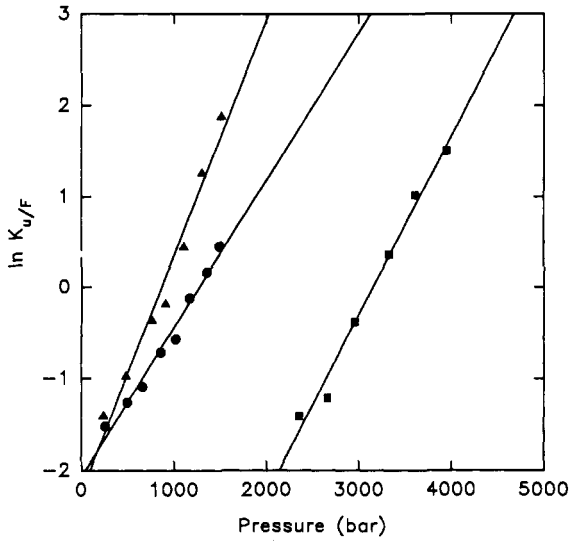

FIGURE 8: Plot of ln $K_{U/F}$ (calculated from NMR $^1H^{\epsilon 1}$ peak integrals) as a function of pressure for (●) WT, (■) H124L, and (▲) H124L+G79S.

Table II: Results of High-Pressure Unfolding of Staphylococcal Nuclease Variants As Observed by ^1H NMR[a]

sample	$\Delta V°$ (mL mol^{-1})	$P_{1/2}$ (bar)	$\Delta G°$ (kcal mol^{-1})
WT nuclease	−53 ± 11	925	−1.2
H124L	−65 ± 7	3109	−4.9
H124L+G79S	−47 ± 3	1195	−1.4

[a] $\Delta V°$ and $\Delta G°$ were calculated at P = 1 bar and T = 310 K from eq 1. $P_{1/2}$ is the pressure at which the protein is half-denatured. Conditions were 10 mM Bis-Tris, pH* 5.1 at 37 °C, in ^2H_2O.

ment of Glu[129] by Lys resulted in a considerable decrease in the long lifetime component. Trp[140] (Figure 1, top) is sandwiched between the methylene groups of the two Lys residues, and the carboxylate of Glu[129] interacts with the indole ring hydrogens. These constraints may hold Trp[140] rigidly in place and thus explain the limited local motion as detected by fluorescence anisotropy. Quenching by either or both of the Lys residues would require motions that permit the encounter of a Lys residue ϵ-amino group with the Trp[140] π system during its excited-state lifetime. Mutants D77A and G79S, each of which appears to relax the structure by disrupting interactions between two loops (those containing P117 and G79) that join the two domains of the protein (Figure 1, bottom), also result

Table III: Fluorescence Results of High-Pressure Denaturation of Staphylococcal Nuclease Variants under Conditions Similar to Those of the NMR High-Pressure Experiments[a]

sample	$\Delta V°$ (mL mol^{-1})	$P_{1/2}$ (bar)	$\Delta G°$ (kcal mol^{-1})
WT nuclease	−57 ± 2	1550	−2.35
H124L+G79S	−55 ± 2	1550	−2.30

[a] $\Delta V°$ and $\Delta G°$ are calculated at P = 1 bar and T = 310 K from eq 1. $P_{1/2}$ is the pressure at which the protein is half-denatured. Conditions were 10 mM Bis-Tris, pH* 5.5 at 37 °C, in D_2O.

in a more heterogeneous native state as assessed both by the *cis/trans* equilibrium at position 117 and by the fluorescence decay. However, substitution at position 76 of Phe by Val also results in a smaller *cis/trans* ratio for Pro[117] (Alexandrescu et al., 1990), yet this mutant exhibits only a very small amplitude for the short-lived component. Apparently, subtle packing rearrangements that take place upon substitution at these positions are communicated to the region surrounding Trp[140] through interactions between these loops [see Figure 2a and Hinck et al. (1990)]. Changes at residues 42 and 47 must be transmitted to Trp[140] through the helix containing Lys[110].

Unfolding profiles obtained from NMR and fluorescence were in good agreement and are consistent with the hypothesis that the high-pressure-induced unfolding of nuclease is a global, two-state process. The $\Delta V°$ values obtained for WT and a number of mutants were considerably higher than those observed by Li et al. (1976) for chymotrypsinogen (−31 mL/mol) and lysozyme (−19 mL/mol) and by NMR for lysozyme (near −10 mL/mol) (Samarasinghe et al., 1992) yet similar to those obtained for metmyoglobin denaturation (near −100 mL/mol) (Zipp & Kauzmann, 1973).

Comparison of the high-pressure time-resolved fluorescence and NMR results suggests a correlation between the pressure stability of a particular mutant and its dynamic properties. Of particular interest is the dramatic difference between the pressure behavior of the Pro → Gly mutants and the other nuclease mutants. H124L+P47G+P117G actually showed an *increase* in fluorescence intensity with pressure. The increase in fluorescence may result from the disruption of a ground-state complex of the tryptophan with a nearby quenching group. Such an effect may reflect compression of the folded state allowed by rearrangements brought on by the Pro → Gly mutation. The decrease in fluorescence intensity with pressure of the single Pro → Gly mutants may also result from compression of the protein or a conformational change other than unfolding (or perhaps a combination of compression and unfolding). Therefore, it was not possible to conclusively assign a $\Delta V°$ to these mutants.

Additionally, the Pro → Gly mutations lead to a decrease in the population of conformers in which the tryptophan residue undergoes significant dynamic fluorescence quenching (Figure 2a). This decrease may reflect closer packing of the native state and therefore decreased mobility of side chains. These properties appear to be related to greater stability. H124L+F76V shows anomalous behavior: although it has a smaller $\Delta V°$ and less dynamic quenching of fluorescence, it is considerably less stable to pressure than WT. This discrepancy is most likely due to the large population of molecules with a *trans* prolyl peptide bond at position 117 in H124L+F76V, which has been shown to lead to instability (Alexandrescu et al., 1990). In general, however, one can imagine that closer packing results in a greater number of stabilizing interactions in the protein and therefore increased stability. This increase in interactions would result in a

decrease in chain mobility and a lower probability of populating high-mobility conformers. One of the roles of surface proline residues in protein structures may be to impose restrictions on the degree of packing of the polypeptide chain to allow for motions required for protein function. Recent crystallographic studies of a mutant of T4 lysozyme, in which Ile[3] in the hinge region of the protein was replaced by a Pro, revealed significant differences in packing and in the binding of water to cavities in the structure (Dixon et al., 1992).

Contributions to $\Delta V°$. A number of factors have been proposed to affect the change in partial molar volume that accompanies unfolding. One such determinant is free volume in the folded state that results from imperfect packing. That the internal free volume could contribute significantly to the $\Delta V°$ of unfolding is supported by theoretical calculations involving X-ray crystallographic data for a number of proteins (Rashin et al., 1986). These investigators found that proteins exhibit a relatively large number of cavities, many of which lack crystallographically determined waters. This internal free volume, which can be occupied by water molecules in the unfolded state, must therefore contribute to the negative $\Delta V°$ of unfolding. The unfolding partial molar volume change of nuclease at 21 °C is approximately 0.5% of the total hydrated volume of the folded protein. The magnitudes of the volumes of internal cavities in the series of proteins studied by Rashin et al. (1986) ranged from 0 to 2% of the total volume and are thus of sufficient magnitude to contribute to the $\Delta V°$ of unfolding.

A second factor that may affect $\Delta V°$ is electrostriction (Zipp & Kauzmann, 1973). Electrostriction results from the increased attraction of water molecules around charged groups. It is reasonable to assume that charged groups in proteins will produce similar electrostriction of water molecules. Such electrostriction may be the reason that $\Delta V°$ is negative at the temperatures examined in this study, since buried ion pairs will be allowed to electrostrict water in the unfolded state. However, the fact that the nuclease volume changes are independent of pH between 7 and 3.5 suggests that electrostriction of water by charges formed by the dissociation of ion pairs upon denaturation does not significantly contribute to $\Delta V°$. In H124L+D77A, the partially buried ion pair between D77 and K78 has been deleted by changing the aspartic acid to an alanine. At a simplistic level of reasoning, if electrostriction by disrupted ion pairs represented a significant contribution to the volume change in the wild-type protein, one would expect that removing an ion pair would lead to a smaller volume change for this mutant. In fact, the volume change for this mutant is the same as that for the wild-type protein. This analysis is not conclusive, however, as there may be compensating effects that mask the contribution of electrostriction.

Another probable contribution to the volume change of denaturation is the decrease in volume upon exposure of buried hydrophobic surfaces to water. Liquid hydrocarbons have a negative $\Delta V°$ for dissolution into water at atmospheric pressure. The magnitude of the dissolution volume, estimated as −0.5 to −2 mL/mol per methylene or methyl group at atmospheric pressure (Taniguchi & Suzuki, 1983), suggests that $\Delta V°$ for protein unfolding should be highly negative on the basis of the large amount of apolar surface exposed. Surprisingly, the dissolution volume of hydrocarbons becomes less negative at higher pressures and eventually turns positive at pressures near 2 kbar (Sawamura et al., 1989). Data from all of the proteins in this study, however, agree with the general observation that $\Delta V°$ for protein folding is constant with pressure. This discrepancy between the pressure behavior of liquid hydrocarbon dissolution and protein denaturation may result from the the higher compressibilities of pure liquid hydrocarbons: nonpolar compounds in pure liquid form are much more compressible than a native protein by approximately a factor of 10 (Kundrot & Richards, 1987). Even so, hydration of exposed hydrophobic residues would nonetheless be of sufficient magnitude to significantly contribute to the $\Delta V°$ of protein unfolding. One therefore expects that mutations that lead to decreased exposure of hydrophobic surface residues in the denatured state, with all else equal, would exhibit smaller volume changes.

Table IV: Comparison of GuHCl Cooperativity Values and Volume Changes for Unfolding[a]

protein	*m* value	$\Delta V°$ (mL mol^{-1})
WT nuclease	1.00	−91.3
H124L+G79S	0.93	−83.8
H124L+D77A	0.90	−89.1
H124L+F76V	1.05	−56.4
H124L+P42G	0.89	*b*
H124L+P47G	0.85	*b*

[a] $m \equiv (\partial \Delta G°/\partial[GuHCl])_{T,P,pH,...}$. All *m* values are normalized to that of Foggi strain staphylococcal nuclease. $\Delta V°$ is calculated at P = 1 bar and T = 294 K from the fluorescence data using eq 1. [b] It was not possible to conclusively determine the $\Delta V°$ values for these mutants (see text).

To examine the hypothesis that nonpolar residues contribute to the negative $\Delta V°$ of unfolding, the *m* values [$m \equiv (\partial \Delta G°/\partial[\mathrm{GuHCl}])_{T,P,pH,...}$] of each mutant were determined. Shortle et al. (1990) have proposed that the *m* value reflects the amount of exposed hydrophobic surface area in the unfolded state, with larger *m* values corresponding to greater exposed hydrophobic surface area in the denatured state. Consequently, one might expect a correlation between *m* value and volume change for unfolding. A comparison of *m* values for GuHCl denaturation and $\Delta V°$ obtained from the fluorescence high-pressure denaturation for the mutants studied here can be found in Table IV. From the limited set of mutants studied here, there does not appear to be a simple correlation between *m* value and the volume change of unfolding. For example, H124L+D77A exhibits a significantly smaller *m* value than WT yet has a comparable volume change, and H124L+F76V exhibits a slightly larger *m* value than WT (Shortle, 1986) yet has a much smaller volume change. Study of a larger set of mutants will be necessary before a conclusion can be made.

The physical basis of the volume change for protein denaturation is highly complex; it involves, at the least, contributions from compressibility, exposure of hydrophobic residues in the native and denatured states, and free volume in the native state. From the data available at present, it is not possible to evaluate the relative weights of these components. A better characterization of the relative importance of factors that contribute to $\Delta V°$ would greatly enhance our understanding of the relationships between structure, packing, dynamics, and stability in polypeptides. The results presented here demonstrate that large differences in $\Delta V°$ result from single amino acid substitutions. Ongoing studies of site-specific mutants with altered cooperativities of GuHCl unfolding and internal free volumes should allow us to begin to differentiate among these various effects.

ACKNOWLEDGMENT

We gratefully acknowledge Dr. P. J. Kraulis for the program MOLSCRIPT (Kraulis, 1991) used in generating the protein

ribbon diagrams of nuclease. C.A.R. thanks Joseph Beechem, Jeanne Rudzki, and Ludwig Brand for communication of their unpublished results.

REFERENCES

Alcala, J. R., Gratton, E., & Prendergast, F. (1987) *Biophys. J. 51*, 925–936.

Alexandrescu, T. A., Ulrich, E. L., & Markley, J. L. (1989) *Biochemistry 28*, 204–211.

Alexandrescu, A. T., Hinck, A. P., & Markley, J. L. (1990) *Biochemistry 29*, 4516–4525.

Anfinsen, C. B. (1973) *Science 181*, 223.

Atkins, W. M., Stayton, P. S., & Villafranca, J. J. (1991) *Biochemistry 30*, 3406–3416.

Ausubel, F. W., Brent, R., Kensington, R. E., Moore, D. D., Seidmen, J. G., Smith, J. A., & Struhl, K. (1987) *Current Protocols in Molecular Biology*, Wiley-Intersciences, New York.

Beechem, J. M. (1992) *Methods Enzymol. 210*, 37–54.

Brandts, J. F., Oliveira, R. J., & Westort, C. (1970) *Biochemistry 9*, 1038–1047.

Chen, L. X.-Q., Longworth, J. W., & Fleming, G. R. (1987) *Biophys. J. 51*, 865–873.

Dill, K. A. (1990) *Biochemistry 29*, 7133–7155.

Dixon, M. M., Nicholson, H., Shewchuk, L., Baase, W. A., & Matthews, B. W. (1992) *J. Mol. Biol. 227*, 917–933.

Eftink, M. R., Gryczynski, I., Wiczk, W., Łackzo, G., & Lakowicz, J. R. (1991a) *Biochemistry 30*, 8945–8953.

Eftink, M. R., Ghiron, C. A., Kautz, R. A., & Fox, R. O. (1991b) *Biochemistry 30*, 1193–1199.

Evans, P. A., Dobson, C. M., Kautz, R. A., Hatfull, G., & Fox, R. O. (1987) *Nature 329*, 266–268.

Evans, P. A., Kautz, R. A., Fox, R. O., & Dobson, C. M. (1989) *Biochemistry 28*, 362–370.

Fox, R. O., Evans, P. A., & Dobson, C. A. (1986) *Nature 320*, 192–194.

Hinck, A. P., Loh, S. N., Wang, J., & Markley, J. L. (1990) *J. Am. Chem. Soc. 112*, 9031–9034.

Hinck, A. P., Eberhardt, E. S., & Markley, J. L. (1993) *Biochemistry* (submitted for publication).

Hutnik, C. M., & Szabo, A. G. (1989) *Biochemistry 28*, 3923–3934.

Jonas, J., Koziol, P., Reiner, C., & Campbell, D. M. (1993) *J. Magn. Reson.* (in press).

Kim, S.-J., Chowdhury, F. N., Stryjewski, W., Ezzat, S. Y., Russo, P. S., & Barkley, M. D. (1993) *Biophys. J.* (in press).

Kraulis, P. (1991) *J. Appl. Crystallog. 24*, 946–950.

Kundrot, C. E., & Richards, F. M. (1987) *J. Mol. Biol. 193*, 157–170.

Kunkel, T. A., Roberts, J. D., & Zakour, R. A. (1987) *Methods Enzymol. 154*, 367–382.

Kuwajima, K., Okayama, N., Yamamoto, K., Ishihara, T., & Sugai, S. (1991) *FEBS Lett. 290*, 135–138.

Li, T. M., Hook, J. W., Drickamer, H. G., & Weber, G. (1976) *Biochemistry 15*, 5572–5581.

Loh, S. N., McNemar, C. W., & Markley, J. L. (1991) *Techniques in Protein Chemistry II*, pp 275–282, Academic Press, New York.

Markley, J. L., Williams, M. N., & Jardetzky, O. (1970) *Proc. Natl. Acad. Sci. U.S.A. 65*, 645–651.

Rashin, A. A., Iofin, M., & Honig, B. (1986) *Biochemistry 25*, 3610–3625.

Rholam, M., Scarlata, S. E., & Weber, G. (1984) *Biochemistry 23*, 6793–6796.

Royer, C. A. (1993) *Anal. Biochem.* (in press).

Royer, C. A., & Beechem, J. M. (1992) *Methods Enzymol. 210*, 481–505.

Royer, C. A., Smith, W. M., & Beechem, J. M. (1991) *Anal. Biochem. 191*, 287–294.

Samarasinghe, S. D., Campbell, D. M., Douglas, M., Jonas, A., & Jonas, J. (1992) *Biochemistry 31*, 7773–7778.

Sambrook, J., Fritsch, E. F., Maniatis, T. (1989) *Molecular Cloning: A Laboratory Manual*, 2nd ed., Cold Spring Harbor Laboratory Press, Cold Spring Harbor, NY.

Sawamura, S., Kitamura, K., & Taniguchi, Y. (1989) *J. Phys. Chem. 93*, 4931–4935.

Scarlata, S. F., Rholam, M., & Weber, G. (1984) *Biochemistry 23*, 6789–6792.

Shalongo, W., Jagannadham, M. V., Heid, P., & Steelwagen, E. (1992) *Biochemistry 31*, 11390–11396.

Shortle, D. (1986) *J. Cell. Biochem. 30*, 281–289.

Shortle, D., Meeker, A. K., & Freire, E. (1988) *Biochemistry 27*, 4761–4768.

Shortle, D., Stites, W. E., & Meeker, A. K. (1990) *Biochemistry 29*, 8033–8041.

Stayton, P. S., & Sligar, S. G. (1991) *Biochemistry 30*, 1845–1851.

Studier, F. W., Rosenberg, A. H., Dunn, J. J., & Dubendorff, J. W. (1989) *Methods Enzymol. 185*, 61–89.

Sugawara, T., Kuwajima, K., & Sugai, S. (1991) *Biochemistry 30*, 2698–2706.

Taniguchi, Y., & Suzuki, K. (1983) *J. Phys. Chem. 87*, 5185.

Valeur, B., & Weber, G. (1977) *Photochem. Photobiol. 25*, 441–444.

Visser, A. J. W. G., Li, T. M., Drickamer, H. G., & Weber, G. (1977) *Biochemistry 16*, 4879–4882.

Wang, J. F., Hinck, A. P., Loh, S. N., LeMaster, D. M., & Markley, J. L. (1990) *Biochemistry 29*, 88–101.

Weber, G., & Drickamer, H. G. (1983) *Q. Rev. Biophys. 16*, 89–112.

Weber, G., Scarlata, S. F., & Rholam, M. (1984) *Biochemistry 23*, 6785–6789.

Zipp, A., & Kauzmann, W. (1973) *Biochemistry 12*, 4217–4228.